FINITE ELEMENT ANALYSIS OF 2-D STRUCTURES BY NEW STRAIN BASED TRIANGULAR ELEMENT

C. Rebiai

Mechanical Engineering Department
University of Batna2
Fésdis, Algeria

ABSTRACT

In this investigation, a new simple triangular strain based membrane element with drilling rotation for 2-D structures analysis is proposed. This new numerical model can be used for linear and dynamic analysis. The triangular element is named SBTE and it has three nodes with three degrees of freedom at each node. The displacements field of this element is based on the assumed functions for the various strains satisfying the compatibility equations. This developed element passed both patch and benchmark tests in the case of bending and shear problems. For the dynamic analysis, lumped mass with implicit/explicit time integration are employed. The obtained numerical results using the developed element converge toward the analytical and numerical solutions in both analyses.

Keywords: Strain approach, Linear analysis, Dynamic analysis, Lumped mass.

1. INTRODUCTION

In recent years, research in plane elements with drilling degrees of freedom has aroused much attention [1-7]. The most important tasks in this research are the improvement of the accuracy and the computational efficiency [8-10]. We note that in FE analysis, the first order displacement based plane elements like constant strain triangle (CST) show poor performance for problems with bending and for plane strain-stress problems, contrarily to the strain based plane elements in which their performances and versatility have been well demonstrated [11]. On the other hand during the last decade, a few number of plane elements based on the strain approach have been developed. It has been proven, that for the plane problems, membrane strain based elements have been found most efficient and suitable. Contrarily for the classical elements with low interpolation terms, the ability of the strain based approach in constructing efficient elements, resulted in decoupling the functions of the various components of insofar as it is allowed by the compatibility equations. This helps in resolving the shear locking phenomena, easy satisfaction of the two main criteria of convergence (rigid body modes and constant strain modes), and the enrichment of the displacements field by higher order terms without introducing non-essential degrees of freedom. So, the main objectives of the strain based approach is to improve the results in terms of accuracy and computing times which has been already demonstrated [12]. While significant attention has been paid to the linear analysis by strain based approach, the modeling of the dynamic part, as also observed in Ref. [13], has not received so much attention. So the success of strain based plane elements recently developed [11-13], the extension of the strain approach to dynamic analysis and in particular to solve problems on contact mechanics, vibration and fatigue [14-17] as well as the significant lack of strain based elements with the mesh distortion effect have motivated this study.

Alternatively, the purpose of this paper is to develop a new triangular element based on the strain field, which could be more suitable for the use in linear and dynamic analysis. This developed element is denoted SBTE (**S**train **B**ased **T**riangular **E**lement) and it is composed of three nodes with three degrees of freedom at each node. It must have a good linear response and be free from locking phenomena, which are a basic prerequisite, for accuracy and high performances. This element is implemented in a computer program written in Fortran language for each case of analysis.

For the purpose of validation, some selected numerical examples with the calculation of deflections, or strains, which are of equal importance, are solved.

2. FORMULATION OF THE ELEMENT

2.1 Strains and Displacements

* Corresponding author (crebiai@yahoo.fr)

DOI : 10.1017/jmech.2018.3
Copyright © 2018 The Society of Theoretical and Applied Mechanics
https://doi.org/10.1017/jmech.2018.3 Published online by Cambridge University Press

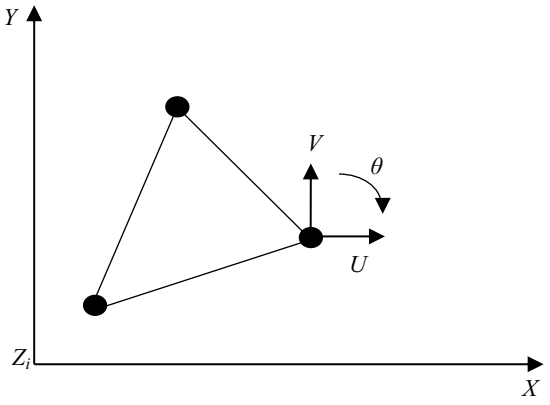


Fig. 1 SBTE element.

We consider the development of this new triangular element which is schematically shown in Fig. 1.

The strain field of the new element SBTE has been enriched by higher order terms in all components of strains in some way to give it good behavior in case of distorted mesh, as compared to SBTIEIR [18] and SBT3 [19]. The procedures for development of the element SBTE follow as below

The three components of strain are given by

$$\begin{Bmatrix} \varepsilon_x \\ \varepsilon_y \\ \gamma_{xy} \end{Bmatrix} = \begin{Bmatrix} \dfrac{\partial U}{\partial x} \\ \dfrac{\partial V}{\partial y} \\ \dfrac{\partial U}{\partial y} + \dfrac{\partial V}{\partial x} \end{Bmatrix} \tag{1}$$

The strains given in Eq. (1) are in terms of two displacements U, V and then they must satisfy the compatibility equations given as below:

$$\frac{\partial^2 \varepsilon_x}{\partial y^2} + \frac{\partial^2 \varepsilon_y}{\partial x^2} - \frac{\partial^2 \gamma_{xy}}{\partial x \partial y} = 0 \tag{2}$$

With all the three strains given by Eq. (1) are equal to zero, and after integrate these equations we obtain the following expressions:

$$\begin{aligned} U &= \alpha_1 - \alpha_3 y \\ V &= \alpha_2 + \alpha_3 x \\ \theta &= \alpha_3 \end{aligned} \tag{3}$$

The zero energy modes of our new strain-based element include the plane rigid body movements given by Eq. (3).

The three displacement coefficients (α_1, α_2, α_3) correspond to rigid body translations and a rigid body rotation respectively. Our element has three nodes with three DOFs at each node, so nine independent coefficients must be in the displacement field of this developed element. Three (α_1, α_2, α_3) are used for the representation of the rigid body components, and the 6 remaining constants (α_4, α_5, …, α_9) are used for expressing the displacement due to straining of the element to give:

$$\begin{aligned} \varepsilon_x &= \alpha_4 + \alpha_5 y + \alpha_9 y^2 \\ \varepsilon_y &= \alpha_6 + \alpha_7 x + \alpha_9 x^2 \\ \gamma_{xy} &= \alpha_8 + 2\alpha_9 (x^2 + y^2 + 2xy) \end{aligned} \tag{4}$$

These strains given by Eq. (4) must satisfy the compatibility equations given by Eq. (2). Expressions (4) are equated to the equations in terms of U, V from Eq. (1) and the resulting equations are integrated, to give:

$$\begin{aligned} U &= \alpha_4 x + \alpha_5 xy - 0.5\alpha_7 y^2 + 0.5\alpha_8 y \\ &\quad + \alpha_9 (xy^2 + 2y^3/3) \\ V &= -0.5\alpha_5 x^2 + \alpha_6 y + \alpha_7 xy + 0.5\alpha_8 x \\ &\quad + \alpha_9 (x^2 y + 2x^3/3) \\ \theta &= -\alpha_5 x + \alpha_7 y + \alpha_9 (x^2 - y^2) \end{aligned} \tag{5}$$

Thus the final displacement functions are obtained by

$$\begin{aligned} U &= \alpha_1 - \alpha_3 y + \alpha_4 x + \alpha_5 xy - 0.5\alpha_7 y^2 + 0.5\alpha_8 y \\ &\quad + \alpha_9 (xy^2 + 2y^3/3) \\ V &= \alpha_2 + \alpha_3 x - 0.5\alpha_5 x^2 + \alpha_6 y + \alpha_7 xy + 0.5\alpha_8 x \\ &\quad + \alpha_9 (x^2 y + 2x^3/3) \\ \theta &= \alpha_3 - \alpha_5 x + \alpha_7 y + \alpha_9 (x^2 - y^2) \end{aligned} \tag{6}$$

2.2 Stresses

The multiplication of elastic matrix [D] by strain vector will give stress vector

$$\sigma = D\varepsilon \tag{7}$$

where

$$\sigma = \{\sigma_x \ \ \sigma_y \ \ \tau_{xy}\}^T \tag{8}$$

In plane stress-strain problems the elasticity matrix [D] is:

$$[D] = \frac{E}{(1-v^2)} \begin{bmatrix} 1 & v & 0 \\ v & 1 & 0 \\ 0 & 0 & \dfrac{1-v}{2} \end{bmatrix} \tag{9}$$

$$[D] = \frac{E}{(1+v)(1-2v)} \begin{bmatrix} 1-v & v & 0 \\ v & 1-v & 0 \\ 0 & 0 & \dfrac{1-2v}{2} \end{bmatrix} \tag{10}$$

2.3 Element Stiffness Matrix

The elementary stiffness matrix [K^e] can be calculated from the well-known expression:

https://doi.org/10.1017/jmech.2018.3 Published online by Cambridge University Press

$$[K^e] = ([C_i]^{-1})^T \left(\int_{-1}^{1} \int_{-1}^{1} [Q]^T [D][Q] \det |J| \, d\xi d\eta \right) [C_i]^{-1} \tag{11}$$

where $[J]$ is the Jacobian of the transformation, $[C_i]$ is the 9 × 9 transformation matrix and $[Q]$ is the strain matrix given respectively by

$$[C_i] = \begin{bmatrix} 1 & 0 & -y_i & x_i & x_i y_i & 0 & -0.5y_i^2 & 0.5y_i & (x_i y_i^2 + 2y_i^3/3) \\ 0 & 1 & x_i & 0 & -0.5x_i^2 & y_i & x_i y_i & 0.5x_i & (x_i^2 y_i + 2x_i^3/3) \\ 0 & 0 & 0 & 0 & -x_i & 0 & y_i & 0 & (x_i^2 - y_i^2) \end{bmatrix} \tag{12}$$

Where x_i and y_i are the coordinates of node i (i = 1, 3).
and

$$[Q] = [L][C] = \begin{bmatrix} 0 & 0 & 0 & 1 & y & 0 & 0 & 0 & y^2 \\ 0 & 0 & 0 & 0 & 0 & 1 & x & 0 & x^2 \\ 0 & 0 & 0 & 0 & 0 & 0 & 0 & 1 & 2(x^2 + y^2 + 2xy) \end{bmatrix} \tag{13}$$

where $[L]$ is the differential matrix given by

$$[L] = \begin{bmatrix} \frac{\partial}{\partial x} & 0 \\ 0 & \frac{\partial}{\partial y} \\ \frac{\partial}{\partial y} & \frac{\partial}{\partial x} \end{bmatrix} \tag{14}$$

and $$[C] = \begin{bmatrix} 1 & 0 & -y & x & xy & 0 & -0.5y^2 & 0.5y & (xy^2 + 2y^3/3) \\ 0 & 1 & x & 0 & -0.5x^2 & y & xy & 0.5x & (x^2 y + 2x^3/3) \\ 0 & 0 & 0 & 0 & -x & 0 & y & 0 & (x^2 - y^2) \end{bmatrix} \tag{15}$$

Equations (4) can be written in matrix form as:

$$\{\varepsilon\} = \begin{Bmatrix} \varepsilon_x \\ \varepsilon_y \\ \gamma_{xy} \end{Bmatrix} = [Q]\{A\} \tag{16}$$

where each of the ε and γ correspond to normal and shear stresses respectively and $\{A\}$ is the parameters vector $\{\alpha_i\} = 1, \ldots 9.$

3. LINEAR NUMERICAL VALIDATION

Four benchmark problems are presented to demonstrate the level of accuracy of this element. All the elements used in comparison are listed as below:

a) SBQE: The four node strain based quadrilateral element with 12 DOFs [12].
b) SBTIEIR: The three node strain based triangular in-plane element with in-plane rotation with 12 DOFs [18].
c) SBREDR Strain based rectangular element with drilling rotation [11].
d) Q8 and Q4: Standars eight/four-node isoparametric elements with 16/8 DOFs.
e) HQ49β Isostatic quadrilateral membrane finite element with drilling DOFs [3].
f) SBT3 Strain based triangular three nodes [19].
g) S8R: Eight Node compatible biquadratic isoparametric element with reduced integration Abacus code [20].
h) T6: Linear strain triangle with 6 nodes and 12 DOFs.
i) PS5β: Pian and Sumihara's four-node five beta mixed element [21].
j) MAQ: Identical to mixed element [22].

3.1 Patch Test

The patch test is an effective test to prove the performance of the finite element in case of distortion. The geometry, materials and mesh of the beam of patch test is depicted in Fig. 2.

The effect of mesh distortion on finite element accuracy is studied on the simple beam shown in Fig. 2. In

https://doi.org/10.1017/jmech.2018.3 Published online by Cambridge University Press

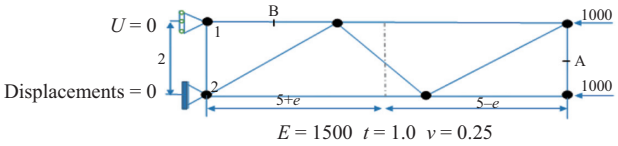


Fig. 2 Cantilever beam: Data and grids.

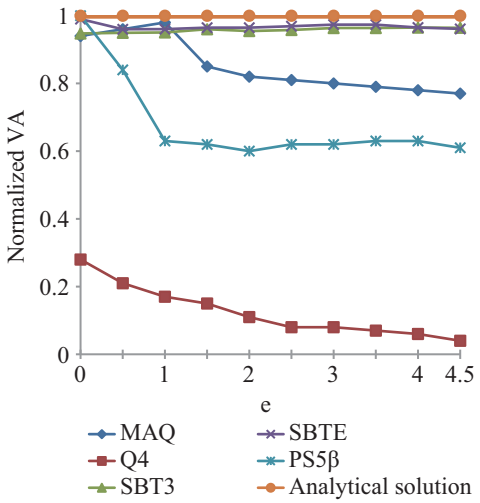


Fig. 3(a) Computed deflections of cantilever beam subjected to end bending $u = 0$ at node 1.

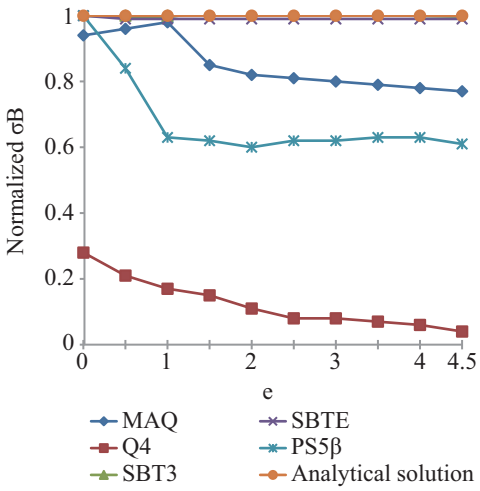


Fig. 3(b) Computed stresses of cantilever beam subjected to end bending $u = 0$ at node 1.

this test used by [23], the simple beam is subjected to end bending. The normalized vertical deflection V_A at point A is plotted against the parameter **e** in Fig. 3(a) and the stresses at point B in Fig. 3(b). By analyzing the displacements, we can see clearly that the results of the developed element is in good agreement with the theoretical values and the element is insensitive to mesh distortion. Concerning the stresses as shown in Fig. 3(b) we can see clearly that SBTE gives good results in terms of stresses and the SBT3 is also good contrarily to other elements.

3.2 Linear Mac-Neal's Elongated Beam

In this example, we consider the standard set of problem suggested by Mac-Neal and Harder [24] in order to evaluate accuracy of the present element. The geometrical and materials characteristics of the beam are shown in Fig. 4.

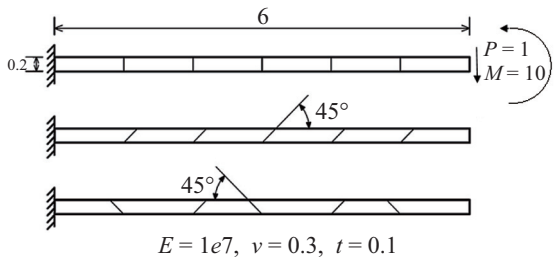


Fig. 4 Mac-Neal and Harder elongated beam test.

The results for selected tests are presented on Table 1. We can see clearly that for the present element, the obtained deflections are in good agreement with the analytical solution in shear and bending, and **SBTE** is insensitive to the mesh distortion in all cases, contrarily to the other elements, which are affected by the distortion effect. The example proves again that the developed element with only 9 DOFs is more economic than the SBQE with 12 DOFs and so it is more efficient in the calculation.

3.3 Cook's Membrane Problem

A tapered panel of unit thickness is subjected to a unit shear load as shown in Fig. 5. The best reference solution is taken from [3, 25]. The deflection of the panel is presented in Table 2. The proposed triangular element is more efficient in this test. It can be seen that the obtained displacement of the SBTE is in closer agreement with the reference solution. Compared with the other elements SBTIEIR, SBT3, S8R and SBQE we can see that SBTE with only 9 DOFs gives a good results, it is more accurate than SBT3 and S8R and more economic than S8R (16 DOFs). Also the developed element exhibits high accuracy in coarse meshes. The SBTE is also more economic than the SBQE (12 DOFs).

3.4 Simple Cantilever Beam

In this example treated in Ref. [26], a cantilever beam (1 × 10 m) as depicted in Fig. 6, supporting at its end a

https://doi.org/10.1017/jmech.2018.3 Published online by Cambridge University Press

Table 1 MacNeal-Harder cantilever beam: Numerical results of deflection for different load cases and mesh geometry.

Elements	Shear $P = 1$						Bending $M = 10$					
	Regular	Error %	Parallel	Error %	Trapezoidal	Error %	Regular	Error %	Prallel	Error %	Trapezoidal	Error %
SBTIEIR	0.0050	95.37	0.0039	96.39	0.000054	99.95	0.0318	88.2	0.0272	89.9	0.0010	99.6
HQ49β	0.1020	5.64	0.0944	12.67	0.0900	16.74	0.255	5.55	0.254	5.92	0.257	4.81
SBTE	**0.1077**	**0.37**	**0.1058**	**2.12**	**0.1058**	**2.12**	**0.269**	**0.37**	**0.268**	**0.74**	**0.268**	**0.74**
SBQE	0.1073	0.74	0.1057	2.22	0.1058	2.12	0.268	0.74	0.266	1.48	0.267	1.11
SBT3	0.1042	3.60	0.1026	5.08	0.1026	5.08	0.267	1.11	0.266	1.48	0.266	1.48
Beam theory	0.1081						0.270					

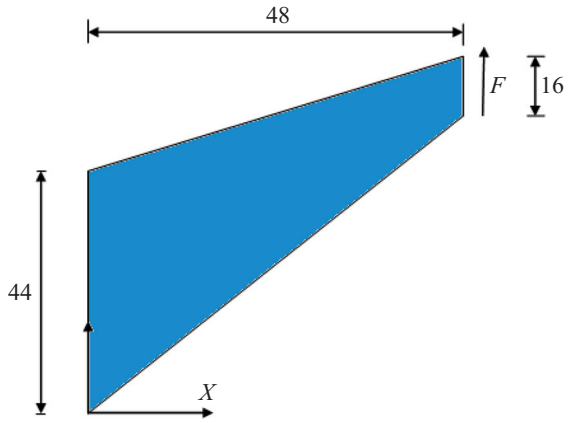


Fig. 5 Cook Tapered panel subjected to shear load.

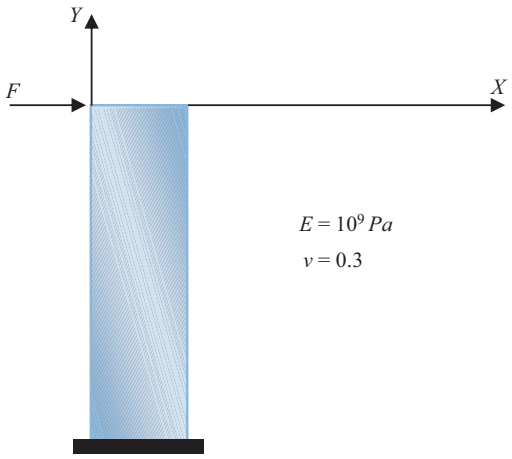


Fig. 6 Cantilever beam subjected to end Load.

Table 2 Deflection of Cook's Panel.

	Load case (1): Force shearing at the free end $P = 1.0$				
Mesh	S8R	SBT3	SBTIEIR	SBQE	**SBTE**
2 × 2	23.05	18.58	17.06	17.87	**18.78**
4 × 4	23.65	23.88	30.64	23.37	**23.94**
8 × 8	23.83	23.88	30.64	23.38	**23.94**
32 × 32	23.93	23.88	30.65	23.50	**23.94**
Error % (mesh 32 × 32)	0.041	0.083	28.20	1.83	**0.0**
Reference solution [3, 19]	1.000 (23.94)				

load of $F = 1000$ N is analyzed. The mesh is (2 × 10) and the computed tip displacements are compared to the slender beam theory and to the others numerical results in Table 3. We can see clearly that the obtained displacement using SBTE is in good agreement with the exact solution. The accuracy and reliability of the developed element makes it better in behaviour than the SBTIEIR in this example. Also the T6 gives a good results but it uses more DOFs than SBTE.

Table 3 Tip displacement of cantilever beam.

Elements	Displacements (m)
SBTE	**3.949×10^{-3}**
SBT3	4.190×10^{-3}
SBTIEIR	3.142×10^{-3}
T6	3.974×10^{-3}
Exact solution [20]	4×10^{-3} (m)

Figures 7 and 8 report the contour and displacements obtained in MacNeal-Harder cantilever beam subjected to bending and shear loads in regular 6 × 1 mesh.

Figure 9 reports the contour and displacements obtained in simple cantilever beam subjected to end loads in 2 × 10 mesh.

4. DYNAMIC NUMERICAL VALIDATION

For this validation three types of problems are considered: eigenvalue problems, forced vibration problems, and dynamic elastoplastic problems

https://doi.org/10.1017/jmech.2018.3 Published online by Cambridge University Press

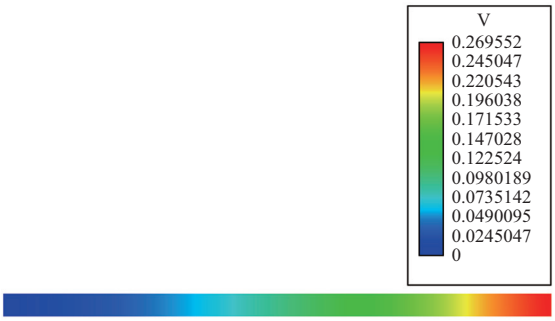


Fig. 7 Mack-Neal beam in bending problem (regular 6 × 1 mesh): Contour and displacements.

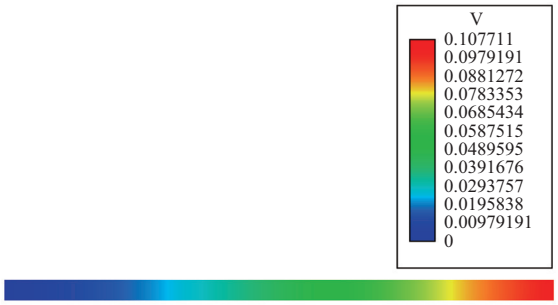


Fig. 8 Mack-Neal beam in shear problem (regular 6 × 1 mesh): Contour and displacements.

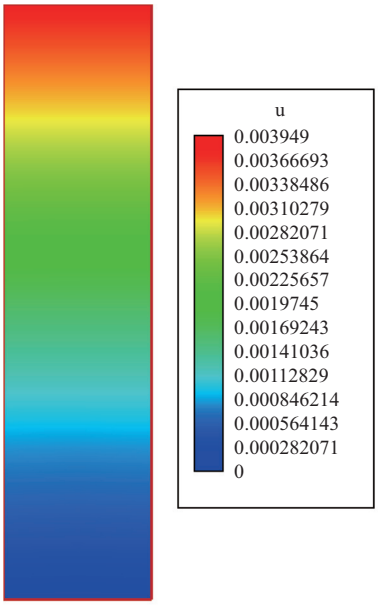


Fig. 9 Contour and displacements of Simple cantilever beam (2 × 10 mesh).

4.1 Eigenvalue Problems

In this test the natural frequencies (fundamental and axial) are computed by solving the linear eigenvalue problem defined by

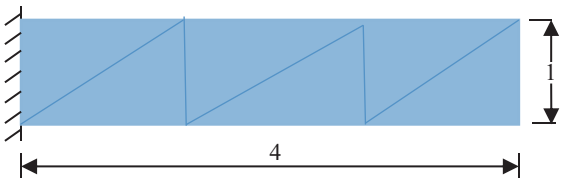


Fig. 10 Geometry and mesh of cantilever beam.

Table 4 Eigenvalues of a cantilever beam

Frequencies		Q4	Q8	**SBTE**
Mesh (3 × 1)	ω_1	0.080	0.064	**0.0594**
	ω_2	0.354	0.413	**0.392**
Mesh (5 × 1)	ω_1	0.068	0.060	**0.063**
	ω_2	0.391	0.391	**0.393**
Mesh (10 × 1)	ω_1	0.062	0.063	**0.063**
	ω_2	0.392	0.391	**0.393**
Error % (5 × 1)	ω_1	7.93	4.76	**0.0**
	ω_2	0.50	0.50	**0.0**
Exact Solution [20]	ω_1	0.063		
	ω_2	0.393		

$$[K_m]\{X\} - \omega^2 [M_m]\{X\} = 0 \tag{17}$$

Where $[K_m]$ is the system stiffness, $[M_m]$ is the mass matrix, ω^2 is the square of the natural frequencies and $\{X\}$ is the displacements vector. The developed element is used to compute the fundamental and axial frequencies and the obtained results are compared with analytical and numerical solutions.

4.1.1 Eigenvalues of Cantilever Beam

This test as depicted in Fig. 10 has been used in several Refs. [26, 27] representing a rectangular cantilever beam with lumped mass, flexural rigidity of 1/12 and Poisson's ratio of 0.3.

The obtained eigenvalues are shown in Table 4. The fundamental frequency ω_1 and the axial frequency ω_2 are computed with different numerical models (Q4, Q8, and SBTE). The obtained results (ω_1 ω_2) by the proposed element are in closer agreement with those obtained by the analytical solution in both cases of mesh (5 × 1 et 10 × 1). The obtained fundamental frequency using the Q4 is considerably higher than that of the analytical solution. Compared to the Q8, which has a high cost and does not reach the exact solution for (ω_2), SBTE is more economic and more accurate.

4.2 Forced Vibration Problems

4.2.1 Forced Vibration of a Cantilever Beam

In order to show the accuracy and performances of the SBTE element in forced vibration, an analysis of beams is performed. A forced vibration analysis of a cantilever beam in plane strain conditions is presented. Both lumped mass, modal superposition method and theta method are used. The same beam is subjected to a

https://doi.org/10.1017/jmech.2018.3 Published online by Cambridge University Press

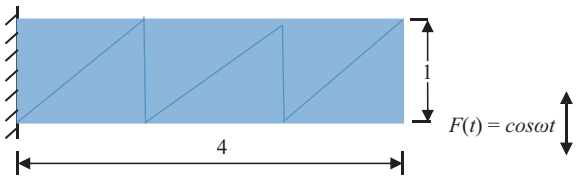


Fig. 11 Geometry and mesh of cantilever beam.

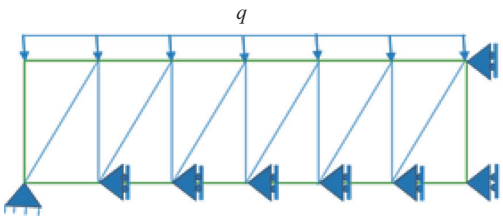


Fig. 12 Geometry and mesh of elasto-plastic beam.

Table 5 Tip displacements of a cantilever beam

	Tip Displacements					
Time (Istep = 20)	Modal Superposition Method			Theta Method		
	Q8	SBREDR	**SBTE**	Q8	SBREDR	**SBTE**
0.1466 + 02	43.22	42.45	**41.76**	2.633	49.14	**48.69**
relative Error % to the Q8 (45.59)	/	1.78	**3.37**	/	7.78	**6.79**

harmonic vertical force cos ωt at the end of the beam Fig. 11, with the same mesh and with a damping ratio of 5% applied to all modes and the forcing frequency is set to 0.3.

From the beam tip displacements in Table 5, it can be seen that the tip displacement obtained at a phase shift of the order of 90° by using SBTE is in good agreement with those obtained by Q8 and SBREDR. However, as it is mentioned in Ref. [26], the obtained amplitude displacement by the Q8 using theta method will be average 45.59, and converges to the solution after 200 time steps once the response has settled down.

4.3 Dynamic Elastoplastic Analysis

4.3.1 Forced Vibration of Elastoplastic Beam

In this example treated in Ref. [27], A beam of (15 × 1) meters, under plane strain conditions as shown in Fig. 12 is analyzed. The numerical data are: $\sigma_{max} = 5 \times 10^7$ Pa, $E = 3 \times 10^{10}$ Pa, $\nu = 0.3$, load $q = 180 \times 10^3$ Pa, the number of time steps is 600. This FEM analysis is performed by lumped mass and the explicit integration scheme. The results presented in Table 6 show the displacements at the upper surface centerline of the beam versus time-steps, the two elements Q8 and SBTE are used in this analysis. The numerical obtained results listed in Table 6, show clearly that the displacements of the SBTE are in good agreement with those obtained by the Q8 [27], especially in last time step in wich the error is between 2% and 3%. The important advantage of the SBTE is that it uses only 9 DOFs, so it is more economic. We note also that the SBTE has a good computational efficiency in this type of analysis.

Figures 13 and 14 report the contour and eigenvalues obtained in case of mesh (3 × 1) of beam and Tip displacements and mesh (6 × 2) of elasto-plastic beam.

Table 6 Tip displacements of elastoplastic beam

Time	Displacements		Error %
	Q8	SBTE	
0	0	0	0
$0.5000.10^{-4}$	$-0.2995.10^{-3}$	$-0.2623.10^{-3}$	12.42
$0.1000.10^{-3}$	$-0.1214.10^{-2}$	$-0.1416.10^{-2}$	16.63
$0.1500.10^{-3}$	$-0.2684.10^{-2}$	$-0.3376.10^{-2}$	25.78
$0.2000.10^{-3}$	$-0.4867.10^{-2}$	$-0.5979.10^{-2}$	22.84
$0.2500.10^{-3}$	$-0.8084.10^{-2}$	$-0.9114.10^{-2}$	12.74
$0.3000.10^{-3}$	$-0.1231.10^{-1}$	$-0.1274.10^{-1}$	3.49
$0.3500.10^{-3}$	$-0.1742.10^{-1}$	$-0.1720.10^{-1}$	1.26
$0.4000.10^{-3}$	$-0.2331.10^{-1}$	$-0.2271.10^{-1}$	2.57
$0.4500.10^{-3}$	$-0.2991.10^{-1}$	$-0.2906.10^{-1}$	2.84
$0.5000.10^{-3}$	$-0.3724.10^{-1}$	$-0.3611.10^{-1}$	3.03
$0.5500.10^{-3}$	$-0.4494.10^{-1}$	$-0.4353.10^{-1}$	3.13
$0.6000.10^{-3}$	$-0.5287.10^{-1}$	$-0.5100.10^{-1}$	3.53

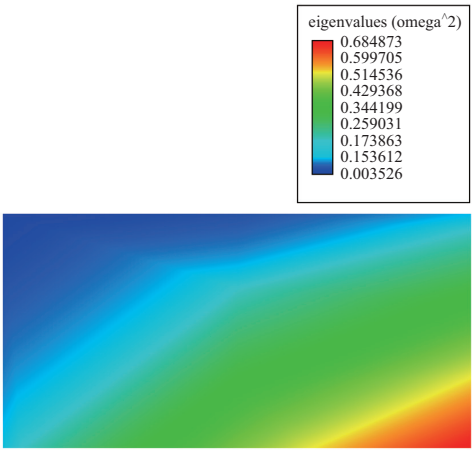


Fig. 13 Cantilever beam: contour and Eigenvalues.

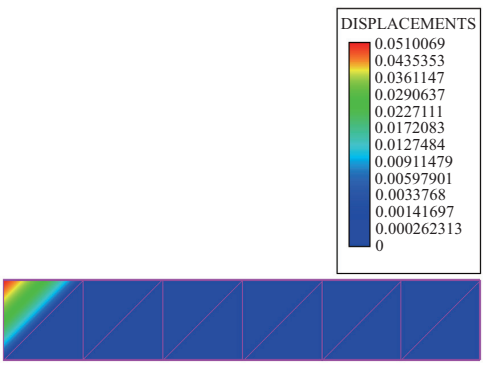


Fig. 14 Elasto-plastic cantilever beam: Contour, mesh and tip displacements.

https://doi.org/10.1017/jmech.2018.3 Published online by Cambridge University Press

5. CONCLUSIONS

In this study, a new strain based triangular element with drilling rotation has been developed and implemented in a computer program written in Fortran language. This element is applied to the linear and dynamic problems under plane stress-strain conditions. Several patch tests and benchmark examples are used to demonstrate the accuracy and the less sensitivity to mesh distortion of this element. As shown by all results, the element is free from locking and it is specified by a good linear response, better than the ones provided by others plan elements especially in the case of mesh distortion. It also behaves better in dynamic problems. This element can be used seriously in the linear and dynamic analysis of plane structures.

REFERENCES

1. Zouari, W., Hammadi, F. and Ayad, R., "Quadrilateral Membrane Finite Elements with Rotational DOFs for the Analysis of Geometrically Linear and Nonlinear Plane Problems," *Computers and Structures*, **173**, pp. 139-149 (2016).
2. Nodargi, N. A. and Bisegna, P., "A Novel High-Performance Mixed Membrane Finite Element for the Analysis of Inelastic Structures," *Computers and Structures*, **182**, pp. 337-353 (2017).
3. Madeo, A., Zagari, G. and Casciaro, R., "An Isostatic Quadrilateral Membrane Finite Element with Drilling Rotations and No Spurious Modes," *Finite Element in Analysis and Design*, **50**, pp. 21-32 (2012).
4. Huang, M., Zhao, Z. and Shen, C., "An Effective Planar Triangular Element with Drilling Rotation," *Finite Element in Analysis and Design*, **46**, pp. 1031-1036 (2010).
5. Belarbi, M. T. and Maalam, T., "On Improved Rectangular Finite Element for Plane Linear Elasticity Analysis," *Revue Européenne des éléments Finis*, **14**, pp. 985-997 (2005).
6. Allman, D. J., "A Quadrilateral Finite Element Including Vertex Rotations for Plane Elasticity Analysis," *International Journal of Numerical Methods in Engineering*, **26**, pp. 717-730 (1988).
7. Kim, J., Varadan, V. V. and Varadan, V. K., "Efficacy of Drilling Degrees of Freedom in the Finite Element Modeling of P-and SV-Wave Scattering Problems," *Journal of Mechanics*, **16**, pp. 103-108 (2000).
8. Ibrahimobigovic, A., Taylor, R. L. and Wilson, E. L., "A Robust Quadrilateral Membrane Finite Element with Drilling Degrees of Freedom," *International Journal of Numerical Methods in Engineering*, **30**, pp. 445-457 (1990).
9. Taylor, R. L. and Simo, J. C., "Bending and Membrane Elements for Analysis of Thick and Thin Shells," *Proceeding of NUMETA Conference, Swansea* (1985).
10. Sheng, G. G. and Wang, X., "The Geometrically Nonlinear Dynamic Responses of Simply Supported Beams under Moving Loads," *Applied Mathematical Modelling*, **48**, pp. 183-195 (2017).
11. Rebiai, C. and Belounar, L., "A New Strain Based Rectangular Finite Element with Drilling Rotation for Linear and Nonlinear Analysis," *Archives of Civil and Mechanical Engineering*, **13**, pp. 72-81 (2013).
12. Rebiai, C. and Belounar, L., "An Effective Quadrilateral Membrane Finite Element Based on the Strain Approach," *Measurement,* **50**, pp. 263-269 (2014).
13. Rebiai, C., Saidani, N. and Bahloul, E., "A New Finite Element Based on the Strain Approach for Linear and Dynamic Analysis," *Research Journal of Applied Science, Engineering and Technology*, **11**, pp. 639-644 (2015).
14. Tang, L., Ding, S., Xie, Y. and Huo, Y., "A Multilayer Nodes Update Method in FEM Simulation of Large Depth Fretting, Wear," *Wear*, **301**, pp. 483-490 (2013).
15. Hu, Z., Lu, W., Thouless, M. D. and Barber, J. R., "Simulation of Wear Evolution Using Fictitious Eigenstrains," *Tribology International*, **82**, pp. 191-194 (2015).
16. Hu, Z., Lu, W., Thouless, M. D. and Barber, J. R., "Effect of Plastic Deformation on the Evolution of Wear and Local Stress Fields in Fretting," *International Journal of Solids and Structures*, **82**, pp. 1-8 (2016).
17. Liu, G. R., Nguyen-Thoi, T. and Lam, K. Y., "An Edge-Based Smoothed Finite Element Method (ES-FEM) for Static, Free and Forced Vibration Analyses of Solids," *Journal of Sound and Vibration*, **320**, pp. 1100-1130 (2009).
18. Sabir, A. B., "A Rectangular and Triangular Plane Elasticity Element with Drilling Degrees of Freedom," *Proceedings of the Second International Conference on Variational Methods in Engineering*, Southampton University, Berlin (1985).
19. Belarbi, M. T. and Bourezane, M., "An Assumed Strain Based on Triangular Element with Drilling Rotation," *Courier de Savoir*, **6**, pp. 117-123 (2005).
20. ABAQUS 6.11., Analysis User's Manual (2011).
21. Pian, T. H. and Sumihara, K., "Rational Approach for Assumed Stress Finite Elements," *International Journal for Numerical Methods in Engineering*, **20**, pp. 1685-1695 (1984).
22. Yunus, S. M., Saigal, S. and Cook, R. D., "On Improved Hybrid Finite Elements with Rotational Degrees of Freedom," *International Journal for Numerical Methods in Engineering*, **28**, pp. 785-800 (1989).
23. Sze, K. Y., Chen, W. and Cheung, Y. K., "An Effi-

https://doi.org/10.1017/jmech.2018.3 Published online by Cambridge University Press

cient Quadrilateral Plane Element with Drilling Degrees of Freedom Using Orthogonal Stress Modes," *Computers & Structures*, **42**, pp. 695-705 (1992).

24. Mac-Neal, R. H. and Harder, R. L., "A Proposed Standard Set of Problems to Test Finite Element Accuracy," *Finite Element in Analysis and Design*, **11**, pp. 3-20 (1985).
25. Cook, R. D., "A Plane Hybrid Element with Rotational Degrees of Freedom and Adjustable Stiffness," *International Journal of Numerical Methods in Engineering*, **24**, pp. 1499-1508 (1987).
26. Smith, I. M. and Griffith, D. V., *Programming the Finite Element Method*, 2nd Edition, John Wiley & Sons, University of Manchester, United Kindom, Hermès (1988).
27. Smith, I. M. and Griffith, D. V., *Programming the Finite Element Method*, 4th Edition, John Wiley & Sons, Ltd, United Kindom (2004).

(Manuscript received August 24, 2017,
accepted for publication January 2, 2018.)

https://doi.org/10.1017/jmech.2018.3 Published online by Cambridge University Press